

Article

Cytotoxic Properties of C₁₇ Polyacetylenes from the Fresh Roots of *Panax ginseng* on Human Epithelial Ovarian Cancer Cells

Ranhee Kim ^{1,†}, So-Ri Son ^{2,†} , Na-Kyung Lee ², Ji-Young Kim ² , Gami An ², Jung-Hye Choi ^{2,3} 
and Dae Sik Jang ^{1,2,*} 

¹ Department of Life and Nanopharmaceutical Sciences, Graduate School, Kyung Hee University, Seoul 02447, Korea

² Department of Biomedical and Pharmaceutical Sciences, Graduate School, Kyung Hee University, Seoul 02447, Korea

³ Department of Oriental Pharmaceutical Science, College of Pharmacy, Kyung Hee University, Seoul 02447, Korea

* Correspondence: dsjang@khu.ac.kr; Tel.: +82-2-9610719

† These authors contributed equally to this work.

Abstract: Although C₁₇ polyacetylenes from *Panax ginseng* exhibit cytotoxic properties against various tumor cells, there have been few experiments on epithelial ovarian carcinoma cells. This study aimed to investigate the cytotoxic effects of C₁₇ polyacetylenes from *P. ginseng* against ovarian cancer cell lines. Four unreported (1–4) and fifteen known (5–19) C₁₇ polyacetylenes were obtained from the roots of *P. ginseng* using repeated chromatography (open column, MPLC, and preparative HPLC). The chemical structures of all the compounds were determined by analyzing their spectroscopic data (NMR, IR, and optical rotation) and HR-MS. The structures of new polyacetylenes were elucidated as (3S,8S,9R,10R)-(-)-heptadeca-9,10-epoxy-4,6-diyne-3,8-diyl diacetate (1), (3S,8S,9R,10R)-(-)-heptadeca-1-en-9,10-epoxy-4,6-diyne-3,8-diyl diacetate (2), (-)-heptadeca-9,10-epoxy-8-methoxy-4,6-diyne-3,11-diol (3), and (3R,9R,10R)-(+)-3-acetoxy-9,10-dihydroxyheptadeca-1-en-4,6-diyne (4), named ginsenoynes O, P, and Q, and 3-acetyl panaxytriol, respectively. Subsequently, in vitro experiments on A2780 and SKOV3 human epithelial ovarian carcinoma cells were performed to assess the cytotoxic properties of the isolates. Among the isolates, panaquinquecol 4 (15) exhibited the most remarkable cytotoxic effects on both human ovarian cancer cells A2780 (IC₅₀ value of 7.60 μM) and SKOV3 (IC₅₀ value of 27.53 μM). Therefore, C₁₇ polyacetylenes derived from *P. ginseng* may warrant further investigation for their therapeutic potential in epithelial ovarian cancer.

Keywords: cytotoxicity; human ovarian cancer; *Panax ginseng*; polyacetylenes



Citation: Kim, R.; Son, S.-R.; Lee, N.-K.; Kim, J.-Y.; An, G.; Choi, J.-H.; Jang, D.S. Cytotoxic Properties of C₁₇ Polyacetylenes from the Fresh Roots of *Panax ginseng* on Human Epithelial Ovarian Cancer Cells. *Molecules* **2022**, *27*, 7027. <https://doi.org/10.3390/molecules27207027>

Academic Editor: Eun Kyoung Seo

Received: 27 September 2022

Accepted: 14 October 2022

Published: 18 October 2022

Publisher's Note: MDPI stays neutral with regard to jurisdictional claims in published maps and institutional affiliations.



Copyright: © 2022 by the authors. Licensee MDPI, Basel, Switzerland. This article is an open access article distributed under the terms and conditions of the Creative Commons Attribution (CC BY) license (<https://creativecommons.org/licenses/by/4.0/>).

1. Introduction

Ovarian cancer, identified as a group of malignant neoplasms, poses a lethal threat to women worldwide [1]. It is the third most common gynecological malignancy, with around 31 million officially recorded cases and 20 million deaths in 2020 [2]. Even the most frequent type of ovarian cancer, epithelial cancer, has a poor prognosis due to the asymptomatic characteristics of its early stages, with a 5-year relative survival rate of only 30% [3,4]. Currently, the common treatment procedure is to first have cytoreductive surgery and to then proceed with platinum-based chemotherapy [5]. However, platinum-based drugs damage normal cells substantially, which can result in organ dysfunction syndrome [6]. Platinum resistance in the treatment of ovarian cancer is also the main factor decreasing survival rate and increasing the risk of relapse [7]. Therefore, novel drugs are urgently required for the effective treatment of ovarian cancer.

Numerous anti-cancer agents derived from traditional medicines have been developed as alternatives to platinum-based chemotherapy with reduced toxic side effects and resistance [8]. *Panax ginseng* Meyer (Araliaceae) and its constituents have anti-tumor effects

in various cancer cell lines, including ovarian cancer [9]. The unique saponin, 20-(S)-ginsenoside Rg3, exhibited anti-tumor effects in ovarian cancer cell lines (SKOV3 and A2780) and in vivo models by inhibiting the Warburg effect caused by reduced lactate synthesis or glucose metabolism [10]. In addition to ginsenosides, a recent review has indicated that C₁₇ polyacetylenes, such as panaxydiol and panaxytriol in *Panax* species, effectively suppress cell proliferation in several cancer cell lines, inducing cell cycle arrest at multi-phases [11]. Although C₁₇ polyacetylenes have potential cytotoxic properties and are abundant among the polyacetylenes found in *P. ginseng*, few investigations on their activity in human ovarian cancer have been conducted. In our preliminary study, we identified the cytotoxic property of polyacetylene-enriched extracts from the fresh roots of *P. ginseng* on epithelial ovarian cancer cells. Therefore, the present research aimed to identify C₁₇ polyacetylenes in *P. ginseng* with cytotoxic effects on human ovarian cancer cell lines.

The present study used repeated chromatography to isolate four newly reported C₁₇ polyacetylenes (1–4) and 15 known compounds (5–19) from a 70% acetone extract of *P. ginseng* roots (Figure 1). The cytotoxicity of the isolated compounds was evaluated in human ovarian cancer cell lines A2780 and SKOV3.

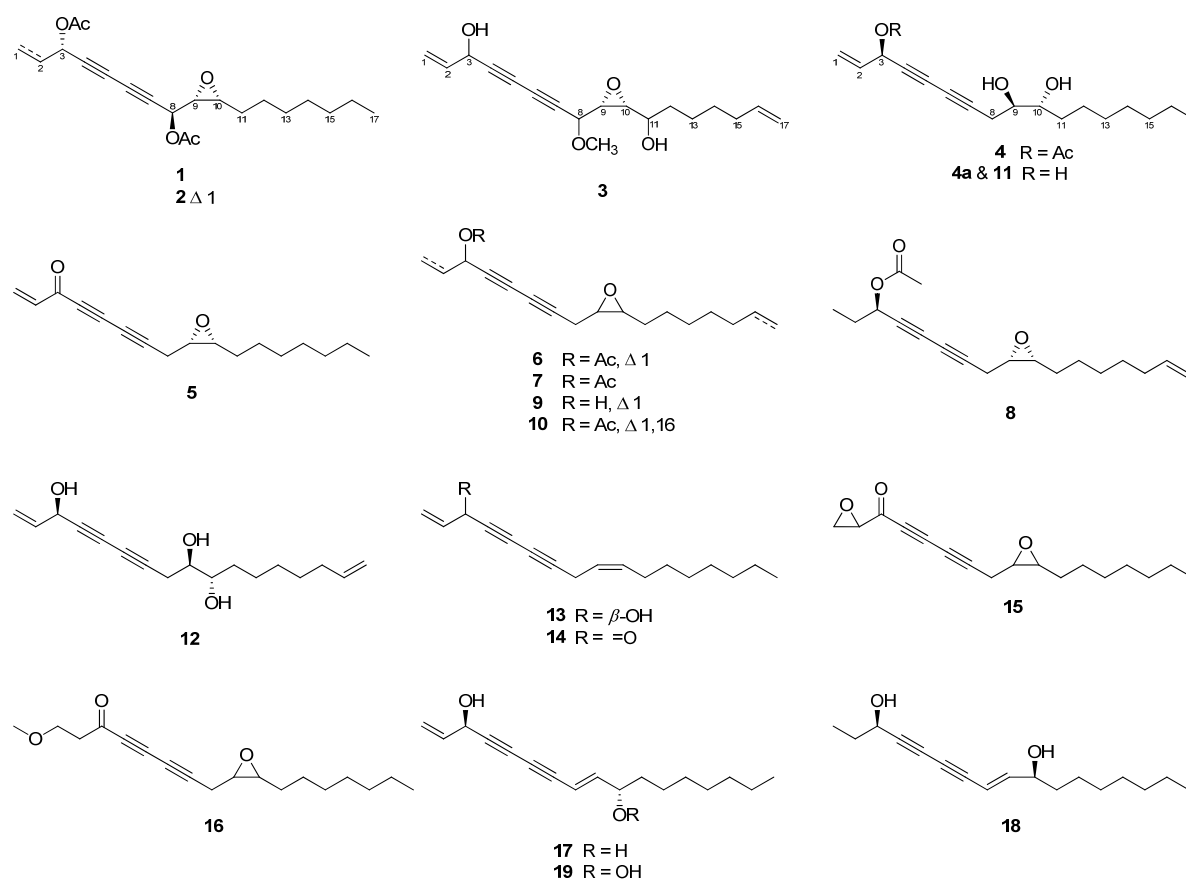


Figure 1. Chemical structures of compounds 1–19 isolated from the roots of *P. ginseng*.

2. Results

2.1. Structure Elucidation of Isolated Compounds

Compound 1 was isolated as yellow oil. The chemical formula was determined to be C₂₁H₃₀O₅ by measuring HR-DART-MS (m/z 380.23495 [M + NH₄]⁺; calcd for C₂₁H₃₄NO₅, 380.24370) (Supplementary Materials Figure S1). The IR spectroscopy exhibited absorption bands at 1380, 1746, and 2250 cm⁻¹, indicating that 1 has a conjugated triple bond and an acetyl group. The ¹H NMR spectrum of 1 suggested the presence of two doublet methyl protons [δ_H 0.88 (3H, t, J = 7.0 Hz, H-17), 1.01 (3H, t, J = 7.5 Hz, H-1)] and two singlet methyl signals [δ_H 2.08 (3H, s, 3-OCOCH₃), 2.11 (3H, s, 8-OCOCH₃)] (Table 1; Figure S2).

Moreover, four oxygenated methine protons at δ_{H} 3.02 (1H, td, $J = 6.0, 4.0$ Hz, H-10), 3.21 (1H, dd, $J = 7.5, 4.0$ Hz, H-9), 5.23 (1H, dd, $J = 7.5, 0.5$ Hz, H-8), and 5.33 (1H, td, $J = 6.5, 0.5$ Hz, H-3) and aliphatic methylene groups at δ_{H} 1.25 (2H, m, H-14), 1.27 (2H, m, H-15), 1.28 (2H, m, H-16), 1.32 (2H, m, H-13), 1.39 (2H, m, H-12), and 1.57 (2H, m, H-11) were identified. Using the HSQC NMR spectrum of **1**, four methyl [δ_{C} 9.5 (C-1), 14.3 (C-17), 20.9 (8-OCOCH₃), 21.1 (3-OCOCH₃)], seven methylene [δ_{C} 22.8 (C-16), 26.7 (C-12), 27.8 (C-11), 28.0 (C-2), 29.4 (C-13), 29.5 (C-14), 32.0 (C-15)], four oxygenated methine [δ_{C} 56.6 (C-9), 58.2 (C-10), 61.9 (C-8), 65.3 (C-3)], four quaternary carbon [δ_{C} 69.3 (C-6), 70.8 (C-5), 74.4 (C-4), 77.7 (C-7)], and two carbonyl signals [δ_{C} 169.1 (8-OCOCH₃), 170.0 (3-OCOCH₃)] were observed (Table 1; Figures S3 and S4). The COSY NMR spectrum revealed correlations between H-1 and H-2/H-3 and between H-8 and H-9/H-10, implying that the methyl, methylene, and oxygenated methine signals are connected (Figure 2 and Figure S5). The HMBC NMR spectrum displayed correlations between H-3 and 3-OCOCH₃/3-OCOCH₃ and between H-8 and C-7/8-OCOCH₃, suggesting that the two acetoxy groups are located at C-3 and C-8 (Figure 2 and Figure S6).

Table 1. ¹H and ¹³C NMR spectroscopic data of compounds **1–3** (δ in ppm, chloroform-*d*).

Position	1		2		3	
	δ_{H} (multi <i>J</i> in Hz) ^a	δ_{C} ^b	δ_{H} (multi <i>J</i> in Hz) ^a	δ_{C} ^c	δ_{H} (multi <i>J</i> in Hz) ^a	δ_{C} ^d
1	1.01 (7.5)	9.5	5.33 d (10.0) 5.52 d (16.5)	120.1	0.99 t (7.5)	9.5
2	1.80 qd (7.5, 6.5)	28.0	5.83 ddd (15.5, 10.0, 6.5)	131.8	1.79 d (6.0)	30.8
3	5.33 td (6.5, 0.5)	65.3	5.88 td (6.5, 1.0)	64.3	4.36 dd (12.0, 6.0)	64.3
4		74.4		74.9		81.2
5		70.8		70.4		72.4
6		69.3		70.5		69.2
7		77.7		75.2		68.8
8	5.23 dd (7.5, 0.5)	61.9	5.22 dd (7.5, 0.5)	61.7	4.01 d (7.0)	70.9
9	3.21 dd (7.5, 4.0)	56.6	3.19 dd (7.5, 4.0)	56.3	3.19 dd (7.5, 4.5)	59.4
10	3.02 td (6.0, 4.0)	58.2	3.00 td (6.0, 3.5)	58.0	2.90 dd (8.5, 4.0)	57.0
11	1.57 m	27.8	1.54 m	26.5	3.40 m	70.0
12	1.39 ^e m	26.7	1.23 ^e	29.7	1.67 m	34.9
13	1.32 ^e m	29.4	1.29 ^e	29.3	1.42 ^e	24.8
14	1.25 ^e m	29.5	1.23 ^e	31.7	1.42 ^e	29.1
15	1.27 ^e m	32.0	1.26 ^e	22.6	2.03 dd (12.5, 5.5)	33.9
16	1.28 m	22.8	1.46	27.6	5.76 ddd (17.0, 10.5, 6.5)	114.7
17a	0.88 t (7.0)	14.3	0.86 t (6.5)	14.1	4.90 ddd (10.0, 2.0, 1.5)	139.0
17b					4.96 ddd (12.0, 2.0, 1.5)	
3-OCOCH ₃	2.08 s	21.1		20.7		
3-OCOCH ₃	-	169.1	2.08 s	168.9		
8-OCOCH ₃	2.11 s	20.9		20.7		
8-OCOCH ₃	-	170.0	2.09 s	169.4		
OMe					3.41 s	57.1

^a The signals were observed at 500 MHz. ^b The signals were observed at 200 MHz. ^c The signals were confirmed by HMBC. ^d The signals were observed at 125 MHz. ^e The signals overlapped.

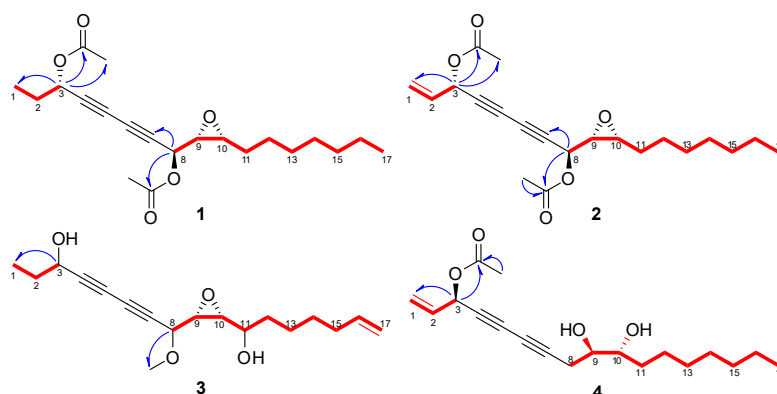


Figure 2. Key ^1H - ^1H COSY (—) and ^1H - ^{13}C HMBC (—) correlations among compounds 1–4.

The relative configuration of **1** was determined by considering the $^3J_{\text{HH}}$ coupling constants and NOESY NMR data. Consistent correlations between H-9 with H-10 and the coupling constants for $^3J_{\text{H9-H10}}$ (4.0 Hz) agreed well with the *cis* configuration [12]. Additionally, the NOESY correlation between H-8 and H-11/H-9 and a large coupling constant for $^3J_{\text{H8-H9}}$ (7.5 Hz) indicated the *erythro* conformation for C-8 and C-9 (Figure 3 and Figure S7) [13,14]. Except for two extra acetyl groups, the structure of **1** was comparable to that of the previously reported (+)-oploxyne A [14,15]. The specific rotation value (-21.4) of **1** was different from that of (+)-oploxyne A. Therefore, the specific rotation value of **1** was calculated based on quantum mechanics using the HF/3-21G* basis set at wavelength 589 nm because sodium D-line was used in the experiments [15]. Four probable absolute configurations of **1** (3*R*/8*S*/9*R*/10*R*, 3*S*/8*S*/9*R*/10*R*, 3*R*/8*R*/9*S*/10*S*, and 3*S*/8*R*/9*S*/10*S*) were modeled and compared with the experimental data of **1**. The calculation result was -12.11 (Table S1), suggesting that the absolute configuration of **1** was 3*S*/8*S*/9*R*/10*R*. Therefore, the chemical structure of **1** was identified as (3*S*,8*S*,9*R*,10*R*)-(-)-heptadeca-9,10-epoxy-4,6-diyne-3,8-diyl diacetate, named ginsenoyne O.

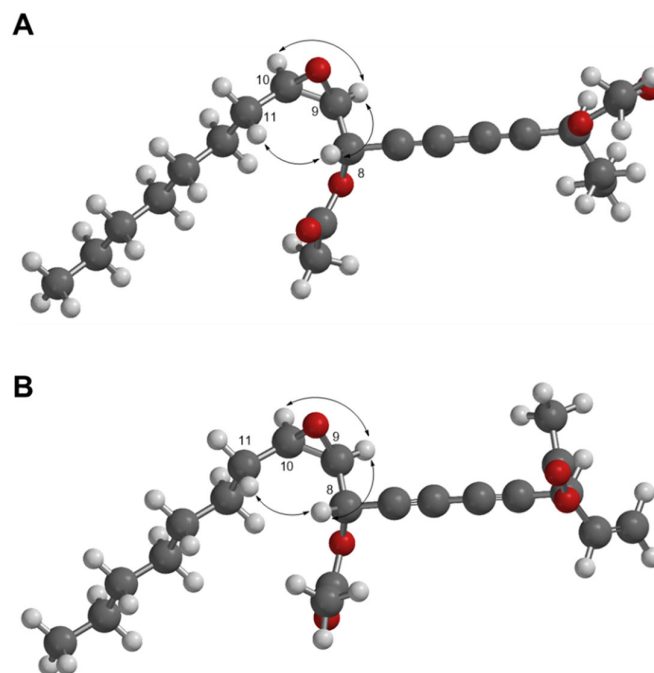


Figure 3. Key NOESY correlations (↪) between compounds **1** and **2** (A,B). The 3D structures of **1** and **2** were modeled by Spartan' 18.

Compound **2** was isolated as yellow oil. The molecular formula of **2** was identified as $\text{C}_{21}\text{H}_{28}\text{O}_5$ by HR-DART-MS (m/z 378.22787 [$\text{M} + \text{NH}_4$] $^+$; calcd for $\text{C}_{21}\text{H}_{32}\text{NO}_5$, 378.22805)

(Figure S8). The IR spectrum showed terminal double bond moiety at 1478 cm^{-1} , acetyl moiety at 1676 cm^{-1} , and triple bond of diyne moiety at 2255 cm^{-1} . The ^1H and DEPT NMR spectra of **2** were similar to **1**, except for the presence of exomethylene signals [δ_{H} 5.33 (1H, d, $J = 10.0\text{ Hz}$, H-1a), 5.52 (1H, d, $J = 16.5\text{ Hz}$, H-1b)]/ δ_{C} 120.1 (C-1) and olefinic signals [δ_{H} 5.83 (1H, ddd, $J = 15.5, 10.0, 6.5\text{ Hz}$, H-2)]/ δ_{C} 131.8 (C-2)] (Table 1; Figures S9 and S10). The above data indicated that **2** was an analog of **1**. The COSY and HMBC experiments led to the determination of the positions for all functional groups in **2** (Figure 2, Figure S11, and Figure S12). The J value analysis ($J_{\text{H9-H10}} = 4.0\text{ Hz}$ / $J_{\text{H8-H9}} = 7.5\text{ Hz}$) and the NOESY correlations suggested that **2** had the same relative configuration as **1** (Table 1; Figure 3 and Figure S13). The absolute configuration of **2** was determined with the same method used for **1** (Table S1). Therefore, the structure of **2** was identified as (3*S*,8*S*,9*R*,10*R*)-(–)-heptadeca-1-en-9,10-epoxy-4,6-diyne-3,8-diyl diacetate, named ginsenoyne P.

Compound **3** was isolated as yellow oil, and its chemical formula was identified as $\text{C}_{18}\text{H}_{26}\text{O}_4$ by HR-DART-MS (Figure S14). Using the MS, IR, and UV data, it was expected that **3** would have a similar structure to **1** and **2**. The ^1H NMR spectrum exhibited an olefinic signal at δ_{H} 5.76 (H-16), five oxygenated methine protons [δ_{H} 2.90 (H-10), 3.19 (H-9), 3.40 (H-11), 4.01 (H-8), and 4.36 (H-3)], exomethylene protons at δ_{H} 4.90 (H-17a) and 4.96 (H-17b), a methyl proton at δ_{H} 0.99 (H-1), and one methoxy signal at δ_{H} 3.41 (8-OCH₃) (Table 1; Figure S15). The ^{13}C and HSQC NMR spectra presented one olefinic carbon at δ_{C} 114.7 (C-16), five oxygenated sp^3 carbons [δ_{C} 57.0 (C-10), 59.4 (C-9), 64.3 (C-3), and 70.9 (C-8)], four sp carbons [δ_{C} 68.8 (C-7), 69.2 (C-6), 72.4 (C-5), and 81.2 (C-4)], one methyl signal at δ_{C} 9.5 (C-1), and one methoxy signal at δ_{C} 57.1 (8-OCH₃) (Table 1; Figures S16 and S17). The connections from C-1 to C-3 and from C-8 to C-17 in **3** were confirmed using an analysis of the COSY data (Figure S18). The position of the methoxy group was determined to be C-8 using an analysis of the HMBC spectrum (Figure 3 and Figure S19). The stereochemistry of the epoxide ring was determined to be *cis* configuration using the J value analysis ($^3J_{\text{H9-H10}} = 4.5\text{ Hz}$). Although the NOESY spectrum exhibited correlations between H-8/H-11 and H-9/H-10 (Figure S20), the relative energies of all conformers exhibited approximate values in the conformer search for **3**. As a highly oxygenated derivative with scarce amount, we could not determine the absolute configuration of **3**. Thus, the structure of **3** was identified as (–)-haptadeca-9,10-epoxy-8-methoxy-4,6-diyne-3,11-diol, named ginsenoyne Q.

Compound **4** was isolated as yellow oil, and its molecular formula was identified as $\text{C}_{19}\text{H}_{28}\text{O}_4$ by HR-DART-MS (Figure S21). The IR spectrum of **4** showed terminal double bond moiety at 1226 cm^{-1} , acetyl moiety at 1746 cm^{-1} , and a triple bond band of diyne moiety at 2307 cm^{-1} . Careful analysis of the ^1H NMR spectrum revealed that the epoxide ring observed in **1–3** was absent in **4** (Figure S22). The ^1H and ^{13}C NMR spectra of **4** were almost identical with those of (3*R*,9*R*,10*R*)-panaxytriol (**11**), which is a major polyacetylene from ginseng and which was also isolated in this study, except for the presence of an acetyl group in **4** (Table 2, Figures S22–S27). The position of the acetyl group in **4** was determined to be C-3 using an analysis of the HMBC spectrum (Figure 2 and Figure S26), implicating that **4** is a different compound from a known 10-acetyl panaxytriol [16]. The coupling constant of H-9 ($^3J_{\text{H9-H10}} = 5.5\text{ Hz}$) in **4** was the same as that of **11**, implicating that they have the same relative configurations at C-9 and C-10. To determine the absolute configuration, deacetylation of **4** was conducted to yield **4a** (Figure S28). The specific rotation value of **4a** (–24.2) was similar to those of **11** (–19.5) and (3*R*,9*R*,10*R*)-panaxytriol in the literature (–18.6) [17], indicating that they have the same absolute configuration. Therefore, the structure of **4** was elucidated as (3*R*,9*R*,10*R*)-(–)-3-acetoxy-9,10-dihydroxyheptadeca-1-en-4,6-diyne, named 3-acetyl panaxytriol.

Table 2. ^1H and ^{13}C NMR spectroscopic data of compound **4** and panaxytriol (**11**) (δ in ppm, chloroform-*d*, 500 and 125 MHz).

Position	4		panaxytriol (11)	
	δ_{H} (multi <i>J</i> in Hz)	δ_{C}	δ_{H} (multi <i>J</i> in Hz)	δ_{C}
1a	5.34 ddd (9.5, 1.0, 1.0)	119.8	5.23 ddd (10.0, 1.0, 1.0)	117.4
1b	5.54 ddd (16.5, 1.0, 1.0)		5.45 ddd (17.0, 1.0, 1.0)	
2	5.86 ddd (16.5, 10.0, 5.0)	132.3	5.92 ddd (17.0, 10.0, 5.0)	136.2
3	5.89 dq (5.5, 1.0)	64.7	4.90 br t (5.0)	63.6
4		71.4		75.0
5		71.6		71.1
6		66.6		66.6
7		78.6		78.3
8a	2.55 ddd (17.5, 5.5, 1.0)	25.1	2.55 ddd (17.5, 6.0, 1.0)	25.8
8b	2.60 ddd (17.0, 6.0, 1.0)		2.59 ddd (17.5, 6.0, 1.0)	
9	3.64 dt (5.5, 5.5)	72.3	3.63 dt (5.5, 5.5)	72.4
10	3.59 dt (5.5)	73.2	3.57 m	73.3
11	1.50 ^a m	34.0	1.48 ^a m	33.7
12a	1.35 ^a m	25.7	1.35 ^a m	25.1
12b	1.46 ^a m		1.45 ^a m	
13	1.27 ^a m	29.7		29.8
14	1.27 ^a m	29.4		29.4
15	1.25 ^a m	32.0	1.22–1.31	32.0
16	1.30 ^a m	22.9		22.9
17	0.88 t (7.0)	14.3	0.87 t (7.0)	14.2
3-OCOCH ₃	2.10 s	21.1		
3-OCOCH ₃		169.8		
9-OH	2.00 br s		2.34 d (5.0)	
10-OH	2.40 br s		2.74 d (5.5)	

^a The signals overlapped.

The structures of the known compounds were identified as ginsenoside E (**5**) [18], acetylpanaxydol (**6**) [19], ginsenoside G (**7**) [20], ginsenoside H (**8**) [20], (3*R*,9*R*,10*S*)-panaxydol (**9**) [21], ginsenoside F (**10**) [20], (3*R*,9*R*,10*R*)-panaxytriol (**11**) [17], ginsenoside C (**12**) [22], panaxynol (**13**) [23], falcarinone (**14**) [24], panaquinquecol 4 (**15**) [25], 1-methoxy-(9*R*,10*S*)-epoxyheptadecan-4,6-diyn-3-one (**16**) [26], (8*E*)-1,8-heptadecadiene-4,6-diyn-3,10-diol (**17**) [21], (3*R*,8*E*,10*S*)-8-heptadecene-4,6-diyn-3,10-diol (**18**) [27], and ginsenoside K (**19**) [21] by comparing their NMR spectroscopic data with those from previously reported studies.

2.2. The Cytotoxicity of C₁₇ Polyacetylenes against Human Ovarian Cancer Cells

To evaluate the effect of the C₁₇ polyacetylenes isolated in this study on the viability of ovarian cancer cells, MTT assay was performed on A2780 and SKOV3 human ovarian cancer cells. As shown in Figure 4 and Table 3, ginsenoside O (**1**), ginsenoside P (**2**), 3-acetyl panaxytriol (**4**), acetylpanaxydol (**6**), ginsenoside G (**7**), (3*R*,9*R*,10*S*)-panaxydol (**9**), ginsenoside F (**10**), (3*R*,9*R*,10*R*)-panaxytriol (**11**), ginsenoside C (**12**), panaxynol (**13**), panaquinquecol 4 (**15**), and 1-methoxy-(9*R*,10*S*)-epoxyheptadecan-4,6-diyn-3-one (**16**) significantly inhibited the viability of A2780 cells in a dose-dependent manner. However, only acetylpanaxydol (**6**), (3*R*,9*R*,10*R*)-panaxytriol (**11**), and panaquinquecol 4 (**15**) exhibited remarkable cytotoxic activities against SKOV3 cells with IC₅₀ values below 50 μM (Table 3 and Figure 5). Among these, panaquinquecol 4 (**15**) showed the most potent cytotoxic activity against A2780 and SKOV3 cells with IC₅₀ values of 7.60 ± 1.33 and 27.53 ± 1.22 μM , respectively.

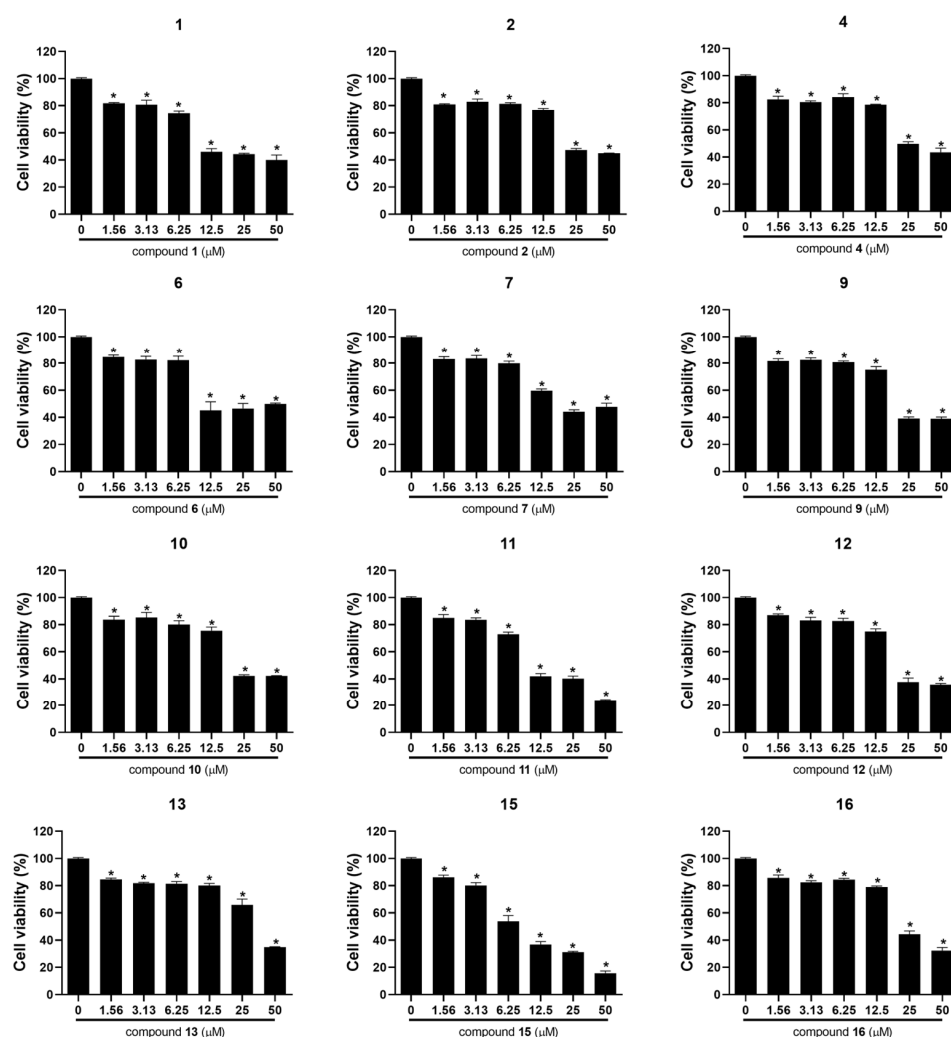


Figure 4. The effects of compounds 1–2, 4, 6–7, 9–13, and 15–16 on cell viability in epithelial ovarian cancer cells A2780. The results are presented as mean standard \pm SD and were processed by using a one-way ANOVA. * $p < 0.05$ in comparison to control (0 μM).

Table 3. The cytotoxicity of compounds 1–19 isolated from *P. ginseng* in A2780 and SKOV3 human ovarian cancer cells.

Compound	IC ₅₀ (μM) ^a		Compound	IC ₅₀ (μM) ^a	
	A2780	SKOV3		A2780	SKOV3
1	11.64 \pm 0.44	>50	11	10.90 \pm 0.25	36.38 \pm 1.95
2	23.86 \pm 0.49	>50	12	20.88 \pm 0.69	>50
3	>50	>50	13	37.63 \pm 1.48	>50
4	25.80 \pm 2.24	>50	14	>50	>50
5	>50	>50	15	7.60 \pm 1.33	27.53 \pm 1.22
6	11.80 \pm 0.81	43.10 \pm 1.15	16	22.96 \pm 0.76	>50
7	20.25 \pm 0.28	>50	17	>50	>50
8	>50	>50	18	>50	>50
9	21.25 \pm 0.12	>50	19	>50	>50
10	22.09 \pm 0.12	>50			

^a IC₅₀ value is the concentration that results in a 50% reduction in cell number when compared to control cultures. Cisplatin used as a positive control. The IC₅₀ value of cisplatin against A2780 and SKOV3 cells were 20.87 \pm 0.94 and 27.65 \pm 0.83 μM , respectively.

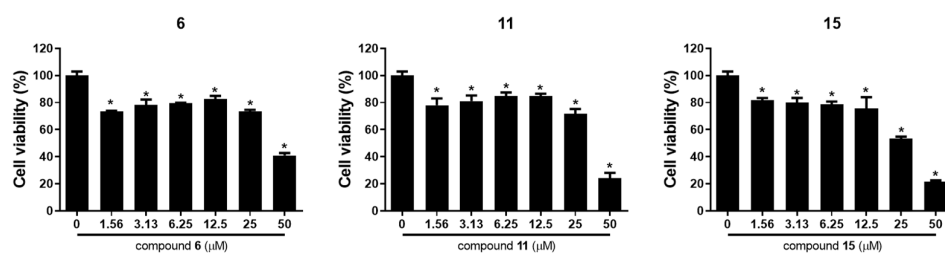


Figure 5. The effects of compounds **6**, **11**, and **15** on cell viability in epithelial ovarian cancer cells SKOV3. The results are presented as mean standard \pm SD and were processed by using a one-way ANOVA. * $p < 0.05$ in comparison to control (0 μM).

Among the isolates, acetylpanaxydol (**6**), (3*R*,9*R*,10*R*)-panaxytriol (**11**), and panaquinquecol 4 (**15**) showed remarkable cytotoxic activities against both ovarian cancer cells (A2780 and SKOV3). To investigate compounds **6**, **11**, and **15** as potential anti-cancer agents by regulating the tumor microenvironments, the cytotoxicity of these compounds was evaluated against RAW264.7 macrophages, the normal cell lines (Table S2). Compounds **11** and **15** showed less cytotoxicity against RAW264.7 (IC_{50} values of 20.03 ± 0.53 and 18.61 ± 0.75 μM , respectively).

3. Discussion

Polyacetylenes, commonly found as secondary metabolites in plants, have one or more carbon-carbon triple bonds in their structure. However, because there are various secondary metabolic pathways involved in the biosynthesis of polyacetylene, these compounds are sometimes highly oxidized and may contain a variety of substituents. Ginseng (*Panax* spp.) is one of the most well-known plants that contains a significant amount of polyacetylene in addition to ginsenosides [28]. For many years, researchers have become more interested in discovering novel ginsenosides as well as polyacetylenes [29]. In this study, four newly reported C17 polyacetylenes—ginsenoyne O, P, and Q (**1–3**), and 3-acetylpanaxytriol (**4**)—were isolated from the fresh roots of *P. ginseng*. Although the presence of panaquinquecol 4 (**15**) and (3*R*,8*E*,10*S*)-8-heptadecene-4,6-diyne-3,10-diol (**18**) was reported in *Panax quinquefolium* and *Oplopanax horridus*, it was reported for the first time in *P. ginseng* in this study.

Epithelial ovarian cancer is classified into several types based on histologic and molecular characteristic [30]. Therefore, high-throughput screening with a variety of epithelial ovarian cancer cell lines is needed for the discovery of selective inhibitors. Polyacetylenes are some of the most significant phytochemicals that contribute to cytotoxic, anti-inflammatory, and potential anti-cancer properties [11,31]. Increasing scientific evidence has shown that panaxdol (**9**) and (3*R*,9*R*,10*R*)-panaxytriol (**11**) are viable anti-cancer drug candidates against epithelial ovarian cancer cells (A2780) as major compounds in *P. ginseng* [32,33]. However, this is the first report that acetylpanaxydol (**6**), ginsenoyne G (**7**), ginsenoyne F (**10**), ginsenoyne C (**12**), panaquinquecol 4 (**15**), and 1-methoxy-(9*R*,10*S*)-epoxyheptadecan-4,6-diyne-3-one (**16**) have cytotoxic effects on ovarian cancer cells.

In this study, the polyacetylenes were more effective against the A2780 cells compared to SKOV3 cells. These results indicated that the p53 pathway is likely associated with compound-induced cell death, and SKOV3 cells without p53 activity seem to be less responsive against the compounds. Nevertheless, panaquinquecol 4 (**15**) exhibited significant cytotoxicity in both A2780 and SKOV3 cells (7.60 ± 1.33 and 27.53 ± 1.22 μM , respectively). It has been reported that panaquinquecol 4 (**15**), which was first isolated from *P. quinquefolium*, has strong cytotoxicity against human leukemia cells (L1210), with an IC_{50} value 20 times lower than panaquinquecol 5, the C₁₄ polyacetylene [25]. However, the cytotoxic effects of panaquinquecol 4 (**15**) against other carcinoma cell lines and their mechanisms are not yet fully understood. Therefore, further investigation into this compound is required.

4. Materials and Methods

4.1. General Experimental Procedure

Thin-layer chromatography (TLC) analysis was performed using RP-18 F254S and silica gel 60 F254 plates (Merck, Kenilworth, NJ, USA). Column chromatography (CC) using Sephadex LH-20 (Amersham Pharmacia Biotech, Buckinghamshire, United Kingdom), Diaion HP-20 (Mitsubishi, Tokyo, Japan), and silica gel (70-230 and 230-400 mesh ASTM, Merck) was implemented to isolate compounds. A medium-pressure liquid chromatography (MPLC) purification system was used with pre-packed cartridges, Redi Sep-C18 and Redi Sep-Silica (Teledyne Isco, Lincoln, NE, USA). Preparative HPLC was performed using the Waters purification system (1525 pump, PDA 1996 detector, Waters, Milford, MA, USA) with Gemini 5 μm NX-C18 110A column (250 \times 21.2 mm i.d., 5.0 μm , Phenomenex, Torrance, CA, USA) and Discovery 5 μm C18 column (250 \times 10.0 mm i.d., 5.0 μm , Supelco, Bellefonte, PA, USA).

The following spectroscopic measurements were obtained for the purified compounds: nuclear magnetic resonance (NMR) spectra using a 500 MHz (JEOL, Tokyo, Japan) and an 800 MHz NMR spectrometer (Bruker, MA, USA); UV spectra using an Optizen pop apparatus (Mecasys, Daejeon, Korea); and optical rotations using a 10 mm microcell on a Jasco P-2000 polarimeter (JASCO, Tokyo, Japan). High-resolution mass spectra (HR-MS) were obtained using an AccuTOF[®] single-reflectron time-of-flight mass spectrometer (JEOL Ltd., Tokyo, Japan) equipped with direct analysis in real-time (DART) ion source (IonSense, Saugus, MA, USA).

4.2. Plant Materials

The fresh roots of *Panax ginseng* C.A. Meyer (Araliaceae) were purchased from a local market (Chungcheongnam-do, Korea) and authenticated by Prof. Dae Sik Jang. A voucher specimen (PAGI-2019) of the raw material was deposited in the Laboratory of Natural Product Medicine, College of Pharmacy, Kyung Hee University, Seoul, Republic of Korea.

4.3. Extraction and Isolation of Polyacetylenes from *P. ginseng*

The sliced raw material (40.53 kg) was extracted with 80 L of 70% acetone for 2 weeks at room temperature, and the solvent was evaporated at 40 °C. The above extraction procedure was repeated once. The 70% acetone extract was then suspended in H₂O (6.4 L) and extracted with EtOAc (6.4 L \times 3) to yield EtOAc- (85.59 g) and water-soluble extracts (772.07 g). The EtOAc-soluble extract was fractionated using silica gel CC (70-230 mesh; ϕ 6.5 \times 48.0 cm) with a gradient system of *n*-hexane-EtOAc (95:5 to 80:20, *v/v*) to yield 24 fractions (E1 ~ E24). E3 (4.08 g) was separated using Sephadex LH-20 CC (ϕ 4.5 \times 55.8 cm) with methylene chloride (MC) to yield nine subfractions (E3-1 ~ E3-9). E3-2 was separated using MPLC with a Redi Sep-Silica cartridge (80 g, *n*-hexane-EtOAc = 100:0 to 75:25 *v/v*) to yield six subfractions (E3-2-1 ~ E3-2-6). E3-2-5 was separated using MPLC with a Redi Sep-C18 gold cartridge (5.5 g, THF-H₂O = 70:30 to 75:25 *v/v*) to afford five subfractions (E3-2-5-1 ~ E3-2-5-5). Compounds **1** (1.0 mg) and **2** (1.0 mg) were purified using semi-prep HPLC with a Discovery column from E3-2-5-1. E3-6 was subjected to a silica gel CC (ϕ 5.0 \times 34.8 cm) with *n*-hexane-EtOAc (from 10:0 to 70:30 *v/v*) to yield eight subfractions (E3-6-1 ~ E3-6-8). Panaxynol (**13**, 658.5 mg), falcarinone (**14**, 67.1 mg), and ginsenoside K (**19**, 15.6 mg) were purified using MPLC with a Redi Sep-C18 cartridge (130 g, acetonitrile-H₂O = 65:35 to 90:10 *v/v*) from E3-6-3. E5 (11.74 g) was subjected to Sephadex LH-20 CC (ϕ 4.5 \times 59.0 cm) with MC to yield five subfractions (E5-1 ~ E5-5). Subfraction E5-4 was separated using silica gel CC (ϕ 5.0 \times 33.3 cm) with *n*-hexane-EtOAc (from 95:5 to 80:20 *v/v*) to yield ginsenoside E (**5**, 48.4 mg) and four subfractions (E5-4-1 ~ E5-4-4). Panaquinquecol **4** (**15**, 4.4 mg) was purified using prep HPLC with a Gemini column from E5-4-3. E5-4-4 was chromatographed using a Redi Sep-Silica cartridge (80 g, *n*-hexane-EtOAc = 100:0 to 70:30 *v/v*) to afford panaxydol (**9**, 430.1 mg) and 1-methoxy-(9*R*,10*S*)-epoxyheptadecan-4,6-diyn-3-one (**16**, 9.1 mg). E2 (2.76 g) was separated using Sephadex LH-20 CC (ϕ 4.8 \times 64.3 cm) with MC to produce six subfractions (E2-1 ~ E2-6).

E2-2 was separated using MPLC with a Redi Sep-Silica cartridge (24 g, MC-acetone = 80:20 to 60:40 *v/v*) to yield eight subfractions (E2-2-1 ~ E2-2-8). E2-2-5 was subjected to MPLC using a Redi Sep-C18 cartridge (26 g, acetonitrile-H₂O = 65:35 to 95:5, *v/v*) to isolate acetylpanaxydol (**6**, 18.6 mg), ginsenoyne G (**7**, 8.6 mg), and ginsenoyne H (**8**, 1.0 mg). E2-2-6 produced ginsenoyne F (**10**, 4.1 mg) by using HPLC with a Gemini column. E14 (8.27 g) was separated into four subfractions (E14-1 ~ E14-4) using Sephadex LH-20 CC (ϕ 4.8 × 64.6 cm) with MC-MeOH = 50:50. Subfraction E14-3 was fractionated using a silica gel CC (ϕ 5.0 × 34.5 cm) with *n*-hexane-EtOAc = 60:40 to afford panaxytriol (**11**, 726.4 mg) and ginsenoyne C (**12**, 5.1 mg). Subfraction E10 (1.15 g) was chromatographed using Sephadex LH-20 CC (ϕ 4.8 × 64.6 cm) with MC-MeOH (70:30, *v/v*) to produce five subfractions (E10-1 ~ E10-5). E10-4 was separated using prep HPLC with a Gemini column to generate (8*E*)-1,8-heptadecadiene-4,6-diyne-3,10-diol (**17**, 4.5 mg) and (3*R*,8*E*,10*S*)-heptadec-8-ene-4,6-diyne-3,10-diol (**18**, 0.7 mg). E12 (436.6 mg) was fractionated using Sephadex LH-20 CC (ϕ 4.8 × 71.0 cm) with MC-MeOH (70:30, *v/v*) to produce seven subfractions (E12-1 ~ E12-7). E12-3 was chromatographed over a Redi Sep-C18 cartridge (26 g, MeOH-H₂O = 60:40 to 80:20 *v/v*) to afford compounds **3** (1.5 mg) and **4** (4.2 mg).

4.3.1. Ginsenoyne O (**1**)

Yellow oil; $[\alpha]_D^{22}$ −21.43; UV (Acetonitrile) λ_{\max} (log ϵ) 233 nm (3.05), 245 nm (2.88), 258 nm (2.70); IR (neat) ν_{\max} 1380, 1746, 2250; DART-MS *m/z* 380.23495 [M + H]⁺ (calcd for C₂₁H₃₁O₅, 380.24370); ¹H and ¹³C NMR data. See Table 1.

4.3.2. Ginsenoyne P (**2**)

Yellow oil; $[\alpha]_D^{22}$ −5.96; UV (Acetonitrile) λ_{\max} (log ϵ) 233 nm (2.99), 246 nm (2.69), 260 nm (2.50); IR (neat) ν_{\max} 1478, 1676, 2255; DART-MS *m/z* 378.22787 [M + NH₄]⁺ (calcd for C₂₁H₃₂NO₅, 378.22805); ¹H and ¹³C NMR data. See Table 1.

4.3.3. Ginsenoyne Q (**3**)

Yellow oil; $[\alpha]_D^{22}$ −4.90; UV (Acetonitrile) λ_{\max} (log ϵ) 224 nm (3.04), 245 nm (2.83), 258 nm (2.72); IR (neat) ν_{\max} 2944, 3003, 3469; DART-MS *m/z* 324.21625 [M + NH₄]⁺ (calcd for C₁₈H₃₀NO₄, 324.21748); ¹H and ¹³C NMR data. See Table 1.

4.3.4. 3-Acetyl Panaxytriol (**4**)

Yellow oil; $[\alpha]_D^{22}$ 33.03; UV (Acetonitrile) λ_{\max} (log ϵ) 222 nm (2.90), 233 nm (2.95), 245 nm (2.82); IR (neat) ν_{\max} 1226, 1746, 2307; DART-MS *m/z* 338.23114 [M + NH₄]⁺ (calcd for C₁₉H₃₂NO₄, 338.23313); ¹H and ¹³C NMR data. See Table 2.

4.4. Computational Chemistry

At the Hartree-Fock level of theory, ab initio calculations for **1** were performed. Using Gaussian 16 software (version G16 C.01; Wallingford, CT, USA) and modified versions of the reported methods, all geometries and conformers of **1** were optimized using an HF/3-21* level of theory [15]. The cumulative Boltzmann distribution (up to 75%, Table S1) was used among generated conformers to select the conformers of **1** for calculating the specific rotation. Specific rotations of single conformers at 589 nm were calculated using a CPCM/HF/3-21* level of theory (chloroform). The final specific rotation value of **1** was calculated using the relative Boltzmann weighting of conformers.

4.5. Deacetylation of Compound **4**

Acid hydrolysis was performed to confirm the absolute configuration of **4** using the modified procedures previously described [34]. Compound **4** (1.0 mg) and 1N HCl (0.01 mL) in MeOH (1.0 mL) were stirred at room temperature for 24 h. After the reaction, it was partitioned with EtOAc and water to obtain a product. The EtOAc fraction was purified directly using HPLC under a gradient system [A: water, B: methanol, 70% B, 35 min].

4.6. Cell Culture and MTT Assay

A2780 and SKOV3 human ovarian cancer cell lines and RAW264.7 macrophages were obtained from American Type Culture Collection (ATCC). The cell culture and MTT assay were performed using the method described previously [35,36].

5. Conclusions

Four new C₁₇ polyacetylenes, ginsenoyne O (**1**), ginsenoyne P (**2**), ginsenoyne Q (**3**), and 3-acetyl panaxytriol (**4**), along with fifteen known ones (**5–19**), were isolated from the fresh roots of *P. ginseng*; moreover, the chemical structures of **1–4** were elucidated using 1D- and 2D- NMR spectroscopy and specific rotation calculation. Among the 19 polyacetylenes, acetylpanaxydol (**6**), (3*R*,9*R*,10*R*)-panaxytriol (**11**), and panaquinquecol 4 (**15**) exhibited a potent cytotoxic effect against both A2780 and SKOV3 human ovarian cells. This finding warrants further investigation into the anti-tumor activity of these C₁₇ polyacetylenes in human ovarian cancer.

Supplementary Materials: The following supporting information can be downloaded at: <https://www.mdpi.com/article/10.3390/molecules27207027/s1>, Figure S1: HR-DART-MS spectrum of compound **1**; Figure S2: ¹H NMR spectrum of compound **1** (500 MHz, chloroform-*d*); Figure S3: ¹³C NMR spectrum of compound **1** (200 MHz, chloroform-*d*); Figure S4: ¹H ¹³C HSQC spectrum of compound **1**; Figure S5: ¹H ¹H COSY spectrum of compound **1**; Figure S6: ¹H ¹³C HMBC spectrum of compound **1**; Figure S7: ¹H ¹H NOESY spectrum of compound **1**; Figure S8: HR-DART-MS spectrum of compound **2**; Figure S9: ¹H NMR spectrum of compound **2** (500 MHz, chloroform-*d*); Figure S10: DEPT NMR spectrum of compound **2** (125 MHz, chloroform-*d*); Figure S11: ¹H ¹H COSY spectrum of compound **2**; Figure S12: ¹H ¹³C HMBC spectrum of compound **2**; Figure S13: ¹H ¹H NOESY spectrum of compound **2**; Figure S14: HR-DART-MS spectrum of compound **3**; Figure S15: ¹H NMR spectrum of compound **3** (500 MHz, chloroform-*d*); Figure S16: ¹³C NMR spectrum of compound **3** (125 MHz, chloroform-*d*); Figure S17: ¹H ¹³C HSQC spectrum of compound **3**; Figure S18: ¹H ¹H COSY spectrum of compound **3**; Figure S19: ¹H ¹³C HMBC spectrum of compound **3**; Figure S20: ¹H ¹H NOESY spectrum of compound **3**; Figure S21: HR-DART-MS spectrum of compound **4**; Figure S22: ¹H NMR spectrum of compound **4** (500 MHz, chloroform-*d*); Figure S23: ¹³C NMR spectrum of compound **4** (125 MHz, chloroform-*d*); Figure S24: ¹H ¹³C HSQC spectrum of compound **4**; Figure S25: ¹H ¹H COSY spectrum of compound **4**; Figure S26: ¹H ¹³C HMBC spectrum of compound **4**; Figure S27: ¹H ¹H NOESY spectrum of compound **4**; Figure S28: ¹H NMR spectra of compounds **11** and **4a**; Table S1. Experimental and calculated specific rotation data of **1** and **2**; Table S2. The cytotoxicity of compounds **6**, **11**, and **15** isolated from *P. ginseng* in RAW264.7 macrophages.

Author Contributions: Conceptualization, D.S.J.; methodology, J.-H.C., S.-R.S. and J.-Y.K.; software, S.-R.S. and J.-Y.K.; investigation, R.K., S.-R.S., N.-K.L., J.-Y.K. and G.A.; writing—original draft preparation, R.K., S.-R.S., N.-K.L. and J.-Y.K.; writing—review and editing, S.-R.S. and J.-Y.K.; visualization, J.-Y.K.; supervision, D.S.J. and J.-H.C.; project administration, D.S.J.; funding acquisition, D.S.J. All authors have read and agreed to the published version of the manuscript.

Funding: This research was funded by a grant from the National Research Foundation of Korea (NRF) funded by the Ministry of Science and ICT (MSIT), Republic of Korea (grant number: NRF–2019R1A2C1083945).

Institutional Review Board Statement: Not applicable.

Informed Consent Statement: Not applicable.

Data Availability Statement: Not applicable.

Conflicts of Interest: The authors declare no conflict of interest.

References

1. Clark, M.A.; Springmann, M.; Hill, J.; Tilman, D. Multiple health and environmental impacts of foods. *Proc. Natl. Acad. Sci. USA* **2019**, *116*, 23357–23362. [[CrossRef](#)] [[PubMed](#)]
2. Sung, H.; Ferlay, J.; Siegel, R.L.; Laversanne, M.; Soerjomataram, I.; Jemal, A.; Bray, F. Global cancer statistics 2020: GLOBOCAN estimates of incidence and mortality worldwide for 36 cancers in 185 countries. *CA Cancer J. Clin.* **2021**, *71*, 209–249. [[CrossRef](#)] [[PubMed](#)]
3. Hurwitz, L.M.; Pinsky, P.F.; Trabert, B. General population screening for ovarian cancer. *Lancet* **2021**, *397*, 2128–2130. [[CrossRef](#)]
4. Kaku, T.; Ogawa, S.; Kawano, Y.; Ohishi, Y.; Kobayashi, H.; Hirakawa, T.; Nakano, H. Histological classification of ovarian cancer. *Med. Electron Microsc.* **2003**, *3*, 9–17. [[CrossRef](#)]
5. Kim, A.; Ueda, Y.; Naka, T.; Enomoto, T. Therapeutic strategies in epithelial ovarian cancer. *J. Exp. Clin. Cancer Res.* **2012**, *31*, 14. [[CrossRef](#)]
6. Oun, R.; Moussa, Y.E.; Wheate, N.J. The side effects of platinum-based chemotherapy drugs: A review for chemists. *Dalton Trans.* **2018**, *47*, 6645–6653. [[CrossRef](#)]
7. Helleman, J.; Smid, M.; Jansen, M.P.; van der Burg, M.E.; Berns, E.M. Pathway analysis of gene lists associated with platinum-based chemotherapy resistance in ovarian cancer: The big picture. *Gynecol. Oncol.* **2010**, *117*, 170–176. [[CrossRef](#)]
8. Mann, J. Natural products in cancer chemotherapy: Past, present and future. *Nat. Rev. Cancer* **2002**, *2*, 143–148. [[CrossRef](#)]
9. Ru, W.; Wang, D.; Xu, Y.; He, X.; Sun, Y.E.; Qian, L.; Zhou, X.; Qin, Y. Chemical constituents and bioactivities of *Panax ginseng* (CA Meyer). *Drug Discov. Ther.* **2015**, *9*, 23–32. [[CrossRef](#)]
10. Yan, Y.B.; Tian, Q.; Zhang, J.F.; Xiang, Y. Antitumor effects and molecular mechanisms of action of natural products in ovarian cancer. *Oncol. Lett.* **2020**, *20*, 141. [[CrossRef](#)]
11. Christensen, L.P. Bioactive C₁₇ and C₁₈ acetylenic oxylinolins from terrestrial plants as potential lead compounds for anticancer drug development. *Molecules* **2020**, *25*, 2568. [[CrossRef](#)]
12. Matsumori, N.; Kaneno, D.; Murata, M.; Nakamura, H.; Tachibana, K. Stereochemical determination of acyclic structures based on carbon-proton spin-coupling constants. A method of configuration analysis for natural products. *J. Org. Chem.* **1999**, *64*, 866–876. [[CrossRef](#)]
13. Yang, M.C.; Kwon, H.C.; Kim, Y.J.; Lee, K.R.; Yang, H.O. Oploxynes A and B, polyacetylenes from the stems of *Oplopanax elatus*. *J. Nat. Prod.* **2010**, *73*, 801–805. [[CrossRef](#)]
14. Yadav, J.; Boyapelly, K.; Alugubelli, S.R.; Pabbaraja, S.; Vangala, J.R.; Kalivendi, S.V. Stereoselective total synthesis of (+)-oploxyne A, (–)-oploxyne B, and their C-10 epimers and structure revision of natural oploxyne B. *J. Org. Chem.* **2011**, *76*, 2568–2576. [[CrossRef](#)]
15. Giorgio, E.; Viglione, R.G.; Zanasi, R.; Rosini, C. Ab initio calculation of optical rotatory dispersion (ORD) curves: A simple and reliable approach to the assignment of the molecular absolute configuration. *J. Am. Chem. Soc.* **2004**, *126*, 12968–12976. [[CrossRef](#)]
16. Kim, S.I.; Lee, Y.H.; Kang, K.S. 10-Acetyl panaxytriol, a new cytotoxic polyacetylene from *Panax ginseng*. *Yakuhak Hoeji* **1989**, *33*, 118–123.
17. Satoh, M.; Ishii, M.; Watanabe, M.; Isobe, K.; Uchiyama, T.; Fujimoto, Y. Absolute structure of panaxytriol. *Chem. Pharm. Bull.* **2002**, *50*, 126–128. [[CrossRef](#)]
18. Hirakura, K.; Morita, M.; Nakajima, K.; Ikeya, Y.; Mitsushashi, H. Polyacetylenes from the roots of *Panax ginseng*. *Phytochemistry* **1991**, *30*, 3327–3333. [[CrossRef](#)]
19. Satoh, M.; Watanabe, M.; Kawahata, M.; Mohri, K.; Yoshida, Y.; Isobe, K.; Fujimoto, Y. Synthesis of panax acetylenes: Chiral syntheses of acetylpanaxydol, PQ-3 and panaxydiol. *Chem. Pharm. Bull.* **2004**, *52*, 418–421. [[CrossRef](#)]
20. Hirakura, K.; Morita, M.; Nakajima, K.; Ikeya, Y.; Mitsushashi, H. Three acetylated polyacetylenes from the roots of *Panax ginseng*. *Phytochemistry* **1991**, *30*, 4053–4055. [[CrossRef](#)]
21. Xu, G.H.; Choo, S.J.; Ryoo, I.J.; Kim, Y.H.; Paek, K.Y.; Yoo, I.D. Polyacetylenes from the tissue cultured adventitious roots of *Panax ginseng* CA Meyer. *Nat. Prod. Sci.* **2008**, *14*, 177–181.
22. Shim, S.Y.; Sung, S.; Lee, M. Ginsenoyne C, a polyacetylene isolated from *Panax Ginseng* inhibit inflammatory mediators via regulating extracellular regulated kinases signaling. *Pharmacogn. Mag.* **2018**, *14*, 358–362.
23. Knispel, N.; Ostrozhenkova, E.; Schramek, N.; Huber, C.; Peña-Rodríguez, L.M.; Bonfill, M.; Palazón, J.; Wischmann, G.; Cusidó, R.M.; Eisenreich, W. Biosynthesis of panaxynol and panaxydol in *Panax ginseng*. *Molecules* **2013**, *18*, 7686–7698. [[CrossRef](#)]
24. Bohlmann, F.; Arndt, C.; Bornowski, H.; Kleine, K. Polyacetylene compounds. XXXI. Polyynes from the family of umbellifers. *Chem. Ber.* **1961**, *94*, 958–967. [[CrossRef](#)]
25. Fujimoto, Y.; Hongcheng, W.; Kirisawa, M.; Satoh, M.; Takeuchi, N. Acetylenes from *Panax quinquefolium*. *Phytochemistry* **1992**, *31*, 3499–3501. [[CrossRef](#)]
26. Lee, S.W.; Kim, K.; Rho, M.C.; Chung, M.Y.; Kim, Y.H.; Lee, S.; Lee, H.S.; Kim, Y.K. New polyacetylenes, DGAT inhibitors from the roots of *Panax ginseng*. *Planta Med.* **2004**, *70*, 197–200. [[PubMed](#)]
27. Ning, J.; Di, Y.T.; Li, S.F.; Geng, Z.L.; He, H.P.; Wang, Y.H.; Wang, Y.Y.; Li, Y.; Li, S.L.; Hao, X.J. Polyynes from *Toona ciliata* var. *ciliata* and related cytotoxic activity. *Helv. Chim. Acta* **2011**, *94*, 376–381. [[CrossRef](#)]
28. Christensen, L.P.; Martin, J.; Ulla, K. Simultaneous determination of ginsenosides and polyacetylenes in American ginseng root (*Panax quinquefolium* L.) by high-performance liquid chromatography. *J. Agric. Food Chem.* **2006**, *54*, 8995–9003. [[CrossRef](#)]
29. Yeo, C.R.; Yong, J.J.; Popovich, D.G. Isolation and characterization of bioactive polyacetylenes *Panax ginseng* Meyer roots. *J. Pharm. Biomed. Anal.* **2017**, *139*, 148–155. [[CrossRef](#)]
30. Rojas, V.; Hirshfield, K.M.; Ganesan, S.; Rodriguez-Rodriguez, L. Molecular characterization of epithelial ovarian cancer: Implications for diagnosis and treatment. *Int. J. Mol. Sci.* **2016**, *17*, 2113. [[CrossRef](#)]

31. Yang, M.C.; Seo, D.S.; Choi, S.U.; Park, Y.H.; Lee, K.R. Polyacetylenes from the roots of cultivated-wild ginseng and their cytotoxicity in vitro. *Arch. Pharm. Res.* **2008**, *31*, 154–159. [[CrossRef](#)]
32. Mao, J.; Zhong, J.; Wang, B.; Jin, J.; Li, S.; Gao, Z.; Yang, H.; Bian, Q. Synthesis of panaxytriol and its stereoisomers as potential antitumor drugs. *Tetrahedron Asymmetry* **2016**, *27*, 330–337. [[CrossRef](#)]
33. Mao, J.; Li, S.; Zhong, J.; Wang, B.; Jin, J.; Gao, Z.; Yang, H.; Bian, Q. Total synthesis of panaxydol and its stereoisomers as potential anticancer agents. *Tetrahedron Asymmetry* **2016**, *27*, 69–77. [[CrossRef](#)]
34. Pollo, L.A.; Bosi, C.F.; Leite, A.S.; Rigotto, C.; Kratz, J.; Simões, C.M.; Fonseca, D.E.; Coimbra, D.; Caramori, G.; Nepel, A. Polyacetylenes from the leaves of *Vernonia scorpioides* (Asteraceae) and their antiproliferative and antiherpetic activities. *Phytochemistry* **2013**, *95*, 375–383. [[CrossRef](#)]
35. Kim, J.Y.; Choi, H.Y.; Kim, H.M.; Choi, J.H.; Jang, D.S. A novel cytotoxic steroidal saponin from the roots of *Asparagus cochinchinensis*. *Plants* **2021**, *10*, 2067. [[CrossRef](#)]
36. Seo, Y.J.; Jeong, M.; Lee, K.T.; Jang, D.S.; Choi, J.H. Isocyperol, isolated from the rhizomes of *Cyperus rotundus*, inhibits LPS-induced inflammatory responses via suppression of the NF- κ B and STAT3 pathways and ROS stress in LPS-stimulated RAW 264.7 cells. *Int. Immunopharmacol.* **2016**, *38*, 61–69. [[CrossRef](#)]